

**NASA Technical Memorandum 107689**

*11. 11. 92  
12. 10. 92  
13. 13*

**Hypersonic Vehicle Control Law  
Development Using  $H_\infty$  and  $\mu$ -Synthesis**

**Irene M. Gregory, Rajiv S. Chowdhry,  
John D. McMinn, and John D. Shaughnessy**

**October 1992**

(NASA-TM-107689) HYPERSONIC  
VEHICLE CONTROL LAW DEVELOPMENT  
USING  $H_\infty$  INFINITY AND  $\mu$ -SYNTHESIS  
(NASA) 13 p

N93-13068

Unclass

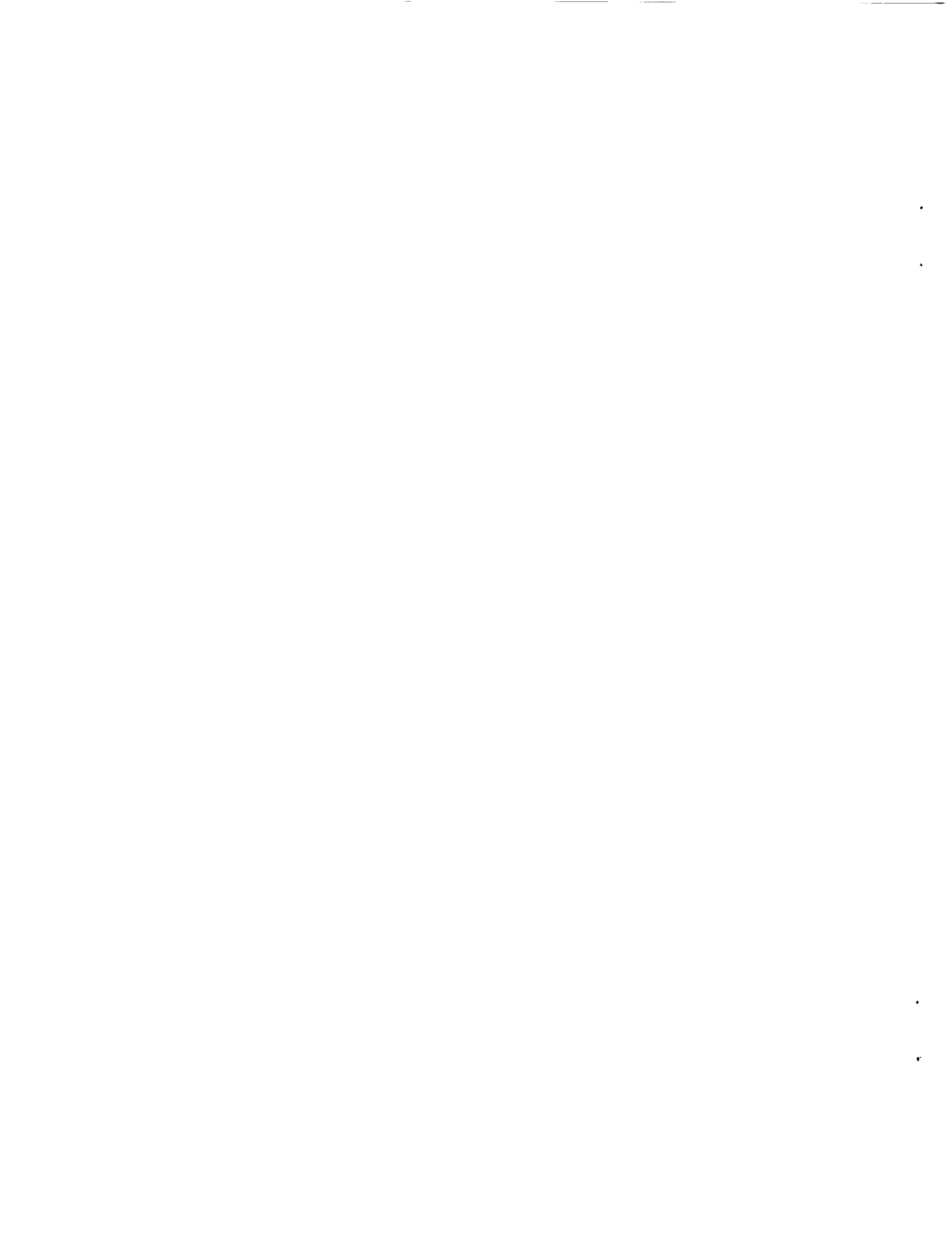
G3/03 0130533



*480308*

National Aeronautics and  
Space Administration

Langley Research Center  
Hampton, Virginia 23665-5225



## Abstract

Applicability and effectiveness of robust control techniques to a single-stage-to-orbit (SSTO) airbreathing hypersonic vehicle on an ascent accelerating path and their effectiveness are explored in this paper. An SSTO control system design problem, requiring high accuracy tracking of velocity and altitude commands while limiting angle of attack oscillations, minimizing control power usage and stabilizing the vehicle all in the presence of atmospheric turbulence and uncertainty in the system, was formulated to compare results of the control designs using  $H_\infty$  and  $\mu$ -synthesis procedures. The math model, an integrated flight/propulsion dynamic model of a conical accelerator class vehicle, was linearized as the vehicle accelerated through Mach 8. Controller analysis was conducted using the singular value technique and the  $\mu$ -analysis approach. Analysis results were obtained in both the frequency and the time domains. The results clearly demonstrate the inherent advantages of the structured singular value framework for this class of problems. Since payload performance margins are so critical for the SSTO mission, it is crucial that adequate stability margins be provided without sacrificing any payload mass.

## 1.0 Introduction

The single-stage-to-orbit (SSTO) airbreathing hypersonic vehicles under consideration present significant challenges in many technological areas and especially in the realm of flight control. They traverse a broader flight envelope than any aircraft flown to date and must emphasize performance during the entire flight regime to achieve their mission objective. Large variations in vehicle static and dynamic characteristics and mass properties, such as significant movement of aerodynamic center of pressure, result in continuously changing static stability margins throughout the flight envelope<sup>1</sup>. Furthermore in general, an additional source of uncertainty arises from the accuracy of mathematical dynamic models used to describe the vehicle in control system design. These challenges and the limited availability of empirical data above Mach 8 in aerodynamics, propulsion, aeroelasticity, heating and on their combined effects on the vehicle's mission performance dictate the need for a robust yet performance oriented control system.

The airframe/propulsion interactions, possibly the most complex of any vehicle, are of critical importance to the hypersonic vehicle mission success. The high sensitivity of the airbreathing propulsion system performance to the changes in angle of attack and dynamic pressure have been identified by Walton<sup>2</sup> and confirmed by Shaughnessy, et al<sup>1</sup>. Furthermore, atmospheric turbulence and especially large density variations at high altitude and Mach number<sup>3</sup> introduce another significant source of uncertainty in the airbreathing propulsion system performance with which the control system must contend.

In addition, as pointed out by Cribbs<sup>4</sup>, uncertainty in parameters, such as propulsive efficiency, drag and vehicle weight, all have major effect on vehicle performance margins in reaching orbital speed. The significantly detrimental effect of control surface deflection induced drag

on the amount of fuel<sup>5</sup> to orbit provides another compelling reason for the importance of the control system optimization in hypersonic class vehicles.

These issues and their impact on the control system development have been previously recognized by a number of researchers, among them Shaughnessy, et al.<sup>1</sup>, McRuer, et al.<sup>6</sup>, Anderson, et al.<sup>7</sup> and others. The control work in this area has primarily addressed the issue of an airbreathing hypersonic cruiser<sup>7</sup> which assumes equilibrium steady state flight with changes in coefficients of the equations of motion stemming from poor model description rather than changing flight parameters due to accelerated flight. Furthermore, the control laws developed for the the ascent phase have either disregarded the impact of angle of attack variations on airbreathing propulsion performance<sup>7</sup> or, while addressing tracking and atmospheric turbulence issues, did not explicitly consider performance robustness<sup>8</sup>.

Recent application of modern robust control theory to the Space Shuttle<sup>9</sup> and fighter aircraft<sup>10</sup> flight control systems demonstrated potential benefits in dealing with the challenges mentioned above. The objective of this research is to assess the applicability and to exploit the capability of modern multivariable robust control theory to explicitly deal with both performance and uncertainty arising from changing flight conditions and vehicle characteristics. The problem is formulated to deal with the challenges associated with an SSTO hypersonic vehicle and its airbreathing propulsion system. A structured uncertainty model, representing parametric variations as actuator uncertainty, is used to compare two modern design procedures,  $H_\infty$  and  $\mu$ -synthesis.

The paper consists of several sections. Section two provides a symbol list and section three gives a brief background review of robustness measures using conventional singular value methods. The issue of possible conservative solutions to some practical problems is discussed and the structured singular value (SSV) is introduced. The theoretical basis for the two synthesis procedures is also provided. This is followed in section four by a five state longitudinal linear model description and its derivation from an ascent trajectory of a conical accelerator class vehicle. Section five provides the problem description which discusses the uncertainty model,  $H_\infty$  weighting function selection, and the explicit inclusion of stochastic atmospheric turbulence in a controller design. The last two sections deal with comparison of  $H_\infty$  and  $\mu$  controller synthesis and analysis techniques as well as the conclusions derived from this study.

## 2.0 Symbols

SSTO	single stage to orbit
$H_\infty$	H infinity norm
$\mu$	structured singular value
$\Delta$	uncertainty matrix
w	uncertainty matrix input vector
e	error/performance vector
z	uncertainty matrix output vector
d	exogenous inputs, i.e. noise, commands, turbulence vector

$P(s)$	generalized plant structure
$K(s)$	controller
$G(s)$	augmented system plant, containing $K(s)$ and $P(s)$
$F_u(G, \Delta)$	perturbed closed loop response between $e$ and $d$
$e'$	generalized output performance vector, $e' = [w \ e]$
$d'$	generalized exogenous input vector, $d' = [z \ d]$
$F_1(P, K)$	closed loop response between $e'$ and $d'$
$u$	control effectors vector
$y$	sensed variables vector
$\ \cdot\ _\infty$	infinity norm
$\sup_\omega$	maximum value over frequency $\omega$
$\bar{\sigma}$	maximum singular value
iff	if and only if
$\ \cdot\ _\mu$	structured singular value over all frequency $\omega$
DOF	degree of freedom
$D$	positive definite Hermitian matrix
$V$	velocity, ft/sec
$\alpha$	inertial angle of attack, deg
$q$	pitch rate, deg/sec
$\theta$	pitch angle, deg
$h$	altitude, ft
$\delta_e$	symmetric elevon
$\dot{m}_f$	fuel mass flow rate
LTI	linear time invariant
$W_\Delta$	uncertainty weighting matrix
$W_{noise}$	measurement noise matrix
$W_p[\cdot]$	performance weighting matrix for a given variable
$a$	bandwidth of elevon dynamics, 25 rad/sec
$b$	bandwidth of fuel flow rate dynamics, 100 rad/sec
$w_i$	unity magnitude white Gaussian noise
$F_{u,w}$	longitudinal and vertical Dryden filters
$[V, h]_c$	commanded velocity and altitude
$[V, h]_{ep}$	performance weighted velocity and altitude error
$[\cdot]_p$	performance weighted variables
$\Delta\delta_e, \Delta\dot{m}_f$	uncertainty in control effectors
$\delta e_c, \delta \dot{m}_{fc}$	controller commanded control inputs
$\delta e_{eff}, \delta \dot{m}_{f\ eff}$	effective control inputs
$\tilde{\delta} e_c, \tilde{\delta} \dot{m}_{fc}$	uncertainty matrix inputs in the general structure
$X_{noise}$	state measurement noise
$\Delta t$	time increment

### 3.0 Theoretical Review of $\mu$

This section provides essential theorems for robustness and performance analysis in a control system with uncertainty. Far more detailed and rigorous discussion is presented in references [11-14].

Analysis methods based on singular values have been successful in providing multiloop extensions for classical single loop techniques<sup>11</sup>. However, these methods are limited to providing exact results, i.e. necessary and sufficient conditions, for robust stability for systems with unstructured uncertainty, defined as norm-bounded but otherwise unknown perturbations. Consider, for example, the standard problem of analyzing a feedback system with simultaneously occurring multiplicative uncertainty at the plant input and output. In order to apply the singular value techniques, both perturbations must be reflected to a single location in the feedback loop, thus immediately inducing conservatism. However, since the combination of linear transformations is linear, any uncertainty occurring at several different locations in the feedback loop can be rearranged as a single block diagonal perturbation in a larger feedback loop. In other words, even unstructured uncertainty at the loop component level becomes highly structured at the system level<sup>12</sup>.

The general framework for the problem is introduced in figure 1a. Any linear combination of inputs, outputs, commands, perturbations and controller can be arranged into the form in the diagram<sup>13</sup>.

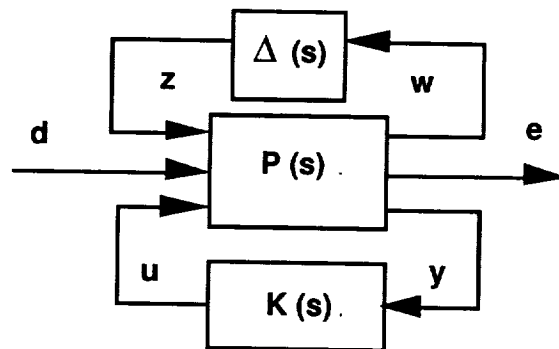


Figure 1a. General Structure

Furthermore, the exogenous inputs  $d$ , the perturbation  $\Delta$  and the output error  $e$  are normalized to 1 with all weightings and scalings absorbed into the generalized plant structure  $P$ . This arrangement results in unit invariant conditions for robust stability and performance expressed in terms of  $\mu$  and presented later in this section. For the purposes of analysis the controller  $K$  can be considered an element of a larger plant  $G$  and be absorbed along with generalized plant  $P$  into its structure. The diagram for the analysis reduces to that in figure 1b.

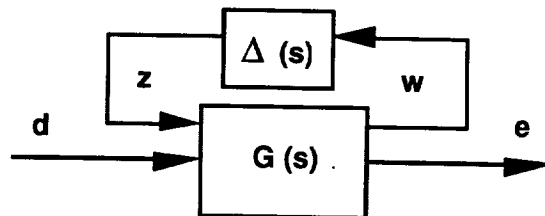


Figure 1b. Analysis Structure

The analysis problem itself involves determining whether the error  $e$  remains in a desired set for sets of inputs  $d$  and uncertainty  $\Delta$ . The resulting structure of  $G$  can be partitioned as

$$\begin{bmatrix} w \\ e \end{bmatrix} = \begin{bmatrix} G_{11} & G_{12} \\ G_{21} & G_{22} \end{bmatrix} \begin{bmatrix} z \\ d \end{bmatrix} \quad (3.1)$$

Closing the upper loop of  $G$  with the uncertainty matrix  $\Delta$  results in a linear fractional transformation given by

$$e = F_u(G, \Delta) d = [G_{22} + G_{21} \Delta (I - G_{11} \Delta)^{-1} G_{12}] d \quad (3.2)$$

The structure for synthesis is similarly given in figure 1c.

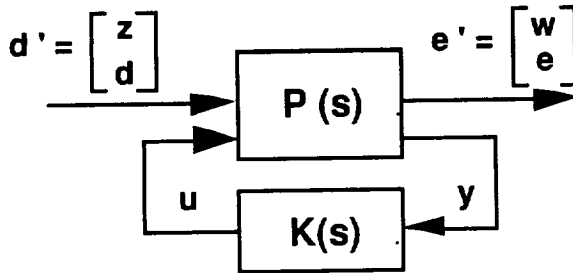


Figure 1c. Synthesis Structure

The inputs and outputs associated with  $\Delta$  are absorbed into the exogenous input  $d'$  and error vector  $e'$ . The equation relating the generalized inputs to outputs is given by

$$e' = F_l(P, K) d' = [P_{11} + P_{12} K (I - P_{22} K)^{-1} P_{21}] d' \quad (3.3)$$

The conditions for stability and performance expressed in terms of  $H_\infty$  bounds on portions of the generalized plant are given and discussed in some detail in references [12-14]. In the absence of uncertainty,  $\Delta$ , the nominal performance objectives are expressed in terms of

$$\|G_{22}\|_\infty \equiv \sup_{\omega} \bar{\sigma}(G_{22}(j\omega)) \leq 1 \quad (3.4)$$

which relates the response  $e$ ,  $\|e\|_2 \leq 1$ , to the set of exogenous inputs  $d$ ,  $\|d\|_2 \leq 1$ . In practice, the use of scalings and weightings is necessary to represent and normalize the varying frequency and spacial content of input and output sets.

Consider plant perturbations that can destabilize a nominally stable system. Robust stability is satisfied for unstructured uncertainty iff the following condition holds,

$$\|G_{11}\|_\infty \leq 1 \quad \text{for all } \Delta, \bar{\sigma}(\Delta) < 1 \quad (3.5)$$

In general for practical problems, the uncertainty consists of parameter variations and multiple norm-bounded perturbations that result from unmodelled dynamics of the system. Parameter variations often arise from changing flight conditions and represent changes in the coefficients of the equations describing the physical system. Unfortunately

the norm-bounded test is insufficient and inadequate in dealing with robust performance and realistic models of plant uncertainty involving structure.

To handle bounded structured uncertainty, the structured singular value (SSV) concept and the function  $\mu$  are used to develop necessary and sufficient conditions<sup>14</sup>. The function  $\mu$  is defined as

$$\mu(M) \equiv \frac{1}{\min_{\Delta \in \Delta} \{\bar{\sigma}(\Delta) \mid \det(I + M\Delta) = 0\}} \quad \text{for } M \in \mathbf{C}^{n \times n} \quad (3.6)$$

unless no  $\Delta \in \Delta$  makes  $I + M\Delta$  singular, in which case  $\mu(M) = 0$ . Based on the definition of  $\mu$  and its properties the robust stability condition is derived. Robust stability is satisfied iff

$$\|G_{11}\|_\mu \equiv \sup_{\omega} \mu[G_{11}(j\omega)] \leq 1 \quad \text{for all } \Delta \in \mathbf{B}\Delta \quad (3.6)$$

with prefix  $\mathbf{B}$  denoting unit ball. Note that, in contrast with  $\bar{\sigma}$ , the value of  $\mu$  is dependent on  $G_{11}$  as well as on the structure of perturbations  $\Delta$ .

The question of interest to the control designer is how well does the system perform in the presence of uncertainty. Consider the issue of robust performance which describes performance with noise and perturbations occurring simultaneously:

$$\begin{aligned} &F_u(G, \Delta) \text{ is stable and } \|F_u(G, \Delta)\|_\infty \leq 1 \\ &\text{for all } \Delta \in \mathbf{B}\Delta \\ &\text{iff } \|G\|_\mu \leq 1 \end{aligned} \quad (3.7)$$

The extreme cases for the structure of  $\Delta$  provide the basis for the computational bounds on  $\mu$ . The structure of  $\Delta$  in general consists of repeated scalar blocks and full matrix blocks.  $\mu$  can be computed exactly from the upper bound if the structure of  $\Delta$  corresponds to  $2S+F \leq 3$ , where  $S$  is the number of repeated scalar blocks and  $F$  is the number of full blocks, thus giving

$$\mu(G) = \inf_{D \in \mathbf{D}} \bar{\sigma}(DGD^{-1}) \quad (3.8)$$

In this particular problem  $\Delta$  consisted of a single repeated scalar block given in a later section. The transformation  $DGD^{-1}$  is essentially a scaling of the inputs and outputs of  $G$  which does not change the value of  $\mu$ . In addition, since  $\mu$  can be computed exactly as a  $\bar{\sigma}$  plus scaling the methods developed for  $H_\infty$  optimal control can be used to optimize  $\mu$ .

$\mu$ -analysis can be combined with  $H_\infty$  optimal control to produce  $\mu$ -synthesis which provides  $H_\infty$  performance in the presence of structured uncertainty. The scaling matrices  $D$  and  $D^{-1}$  are used to reflect the structure of  $\Delta$  over the frequency range. The problem now becomes reformulated as an  $H_\infty$ -norm minimization of

$$\|D F_l(P, K) D^{-1}\|_\infty \leq 1 \quad (3.9)$$

known as D-K iteration. As the D-K name implies, the  $\mu$ -synthesis approach is to iterate between D and K until the solution converges<sup>14</sup>. The method is not guaranteed to produce a global minimum or to converge; however, the results, widely published in literature, have been successful in practical applications.

#### 4.0 Hypersonic Vehicle Model

A conical accelerator configuration was used as an example for a generic airbreathing hypersonic vehicle<sup>15</sup>. As the vehicle accelerated through Mach 8 at 86,000 feet, a ten-state linear model representing the vehicle dynamics was obtained at this non-equilibrium flight condition, which is characterized by non-zero translational and rotational accelerations. The linear model was decoupled into a five-state longitudinal and a five-state lateral-directional model. The five state longitudinal vector  $\mathbf{x}$  and control vector  $\mathbf{u}$ , utilized in this study, are given by

$$\mathbf{x} = [v \ \alpha \ q \ \theta \ h]^T \quad (4.1)$$

$$\mathbf{u} = [\delta_\theta \ \delta \dot{m}_f]^T \quad (4.2)$$

The state and control variables are perturbation quantities and represent deviations from the nominal flight conditions. The open loop characteristics of the plant are unstable. Note that the altitude is included as a state variable to account for temperature, density and gravity gradients. These variations significantly affect the longitudinal long-period dynamics of the vehicle and add an aperiodic altitude mode caused by the variation of atmospheric density with altitude<sup>16</sup>.

Several interesting nuances about this model are worth considering. In all practical problems, a linear time invariant (LTI) system is only an approximation to the real behavior. In most cases, time invariance of the system's characteristics is valid for "small" increments of time as determined by the researcher and dictated by the problem. In this particular case, the vehicle accelerates through Mach 8 and the LTI system is valid for only that instant of time. However, if the parameter variation with time is represented as a multiplicative uncertainty such that  $\tilde{\mathbf{G}} = \mathbf{G} (1 + \Delta)$ , then the linear system can be considered time invariant and can be used in LTI control design.

Secondly, it is important to recognize that air mass flow rate changes almost instantaneously at hypersonic speeds with a change in angle of attack. This relationship is not explicitly included in the original nonlinear model; however, the control problem is formulated to account for the major airframe/propulsion interactions. This is reflected in explicit performance requirements on angle of attack as well as the engine control effector,  $\dot{m}_f$ . For generality and convenience,  $\dot{m}_f$  is expressed in terms of fractional change from the nominal rather than in physical units.

#### 5.0 Problem Description

The controller requirements were established based on the near optimal ascent trajectory and the sensitivity of the airbreathing propulsion system to angle of attack variations. Thus the specifications included high accuracy tracking of velocity and altitude commands while limiting angle of attack total deflection from nominal to 0.5 degrees, minimizing control power use and stabilizing the vehicle all in the presence of atmospheric turbulence and uncertainty in the system. It was assumed for the purposes of this study that  $\mathbf{x}_{state} = \mathbf{y}_{meas}$  and was available for output feedback. The assumption was based on the availability of  $\alpha$  inertial from calculations using outputs from an inertial measurement unit (IMU).

The block diagram problem formulation is illustrated in figure 2a. All feedback state measurements were assumed to be corrupted by noise with the noise matrix represented by

$$\mathbf{W}_{noise} = 10^{-6} \mathbf{I}_5 \quad (5.1)$$

The noise matrix was not intended to represent realistic sensor data and was included because the application of  $H_\infty$  to output feedback requires that the measured signals are corrupted by noise. Furthermore, the control actuator dynamics were represented by first order filters with 25 rad/sec bandwidth for elevon and 100 rad/sec bandwidth for fuel flow rate. In a generic airbreathing hypersonic vehicle, the uncertainty, as discussed above, comes from different sources and occurs simultaneously. Thus, the very physics of the problem impose a structure on an uncertainty of a hypersonic vehicle. In order to explore the effects of structure on  $H_\infty$  and  $\mu$  based analysis and synthesis techniques, actuator uncertainty was chosen for this problem. To represent parameter variation due to acceleration of the vehicle, a 20 percent multiplicative uncertainty,  $\Delta$ , in the control effectiveness was introduced to the system where

$$\Delta = \begin{bmatrix} \delta & 0 \\ 0 & \delta \end{bmatrix} \quad \delta \in \mathbf{C} \quad (5.2)$$

and the uncertainty weighting matrix was

$$\mathbf{W}_\Delta = \begin{bmatrix} 0.2 & 0 \\ 0 & 0.2 \end{bmatrix} \quad (5.3)$$

Thus, the control effectiveness was forced to vary from 80 percent to 120 percent of the assumed nominal. At this stage of problem development, atmospheric density perturbations were assumed to be reflected in the 20 percent uncertainty in fuel flow rate effectiveness.

Performance specifications for a flight control system translate quite well into an  $H_\infty$  context for this problem. In designing for tight performance margins, performance weighting, or penalty functions, were augmented to the system.  $H_\infty$  performance specifications make practical sense only when meaningful variables are specified for weighting functions. As illustrated in figure 2a, the weighting functions for control effector positions and rates as well as for the state vector were employed as output performance variables.

Specific performance requirements were derived from near fuel optimum ascent trajectory for the conical accelerator. The frequency dependent performance weightings are used for velocity and altitude error. The time response requirements for velocity are specified as 10 percent overshoot, translating into 0.5 high frequency gain, 40 sec time constant, giving 0.025 rad/sec as cross-over frequency, and 5 percent steady state error, equivalent to low frequency gain of 50, all of which translate into

$$W_{pV_e} = \frac{0.5 (s + 4.33e-2)}{(s + 4.33e-4)} \quad (5.4)$$

Similarly, altitude time response specifications, 10 percent overshoot, 35 sec time constant, 5 percent steady state error, result in

$$W_{ph_e} = \frac{0.5 (s + 4.95e-2)}{(s + 4.95e-4)} \quad (5.5)$$

Constant weighting was applied to  $\alpha$ ,  $q$  and  $\theta$  resulting in

$$W_p \begin{bmatrix} \alpha \\ q \\ \theta \end{bmatrix} = \begin{bmatrix} 15 \\ 1 \\ 1 \end{bmatrix} \quad (5.6)$$

The weighting for  $\alpha$  was based on the desire to attenuate

atmospheric disturbances and to limit the magnitude of the output as much as possible without violating performance requirements on other variables and was derived by iteration. Similarly actuator position and rate limits were imposed by

$$W_p \begin{bmatrix} \delta e \\ \delta \dot{m}_f \end{bmatrix} = \begin{bmatrix} 25 \\ 60 \end{bmatrix} \quad (5.7)$$

$$W_p \begin{bmatrix} \delta \dot{e} \\ \delta \ddot{m}_f \end{bmatrix} = \begin{bmatrix} 1 \\ 1.5 \end{bmatrix} \quad (5.8)$$

Lastly, atmospheric turbulence is also explicitly included in the problem formulation. The primary concern is the effect of turbulence in engine performance. Turbulence can either affect performance directly by changing inlet flow conditions or by exciting actuator controllers, leading to undesirable vehicle angle of attack variations. Longitudinal and vertical Dryden turbulence filters are implemented as input weighting functions in the generalized framework ( $F_U$  and  $F_W$  in figure 2a)<sup>17, 18</sup>. Filter inputs,  $w_1$  and  $w_2$ , to  $F_U$  and  $F_W$ , respectively, represent white, zero mean, unit variance noise signals. The longitudinal Dryden filter output is assumed to act along the velocity vector due to a small angle of attack flight condition. The vertical Dryden filter is divided by nominal velocity,  $V_0$ , to give angle of attack instead of vertical velocity perturbation. Furthermore, for correct implementation in a discrete simulation environment the

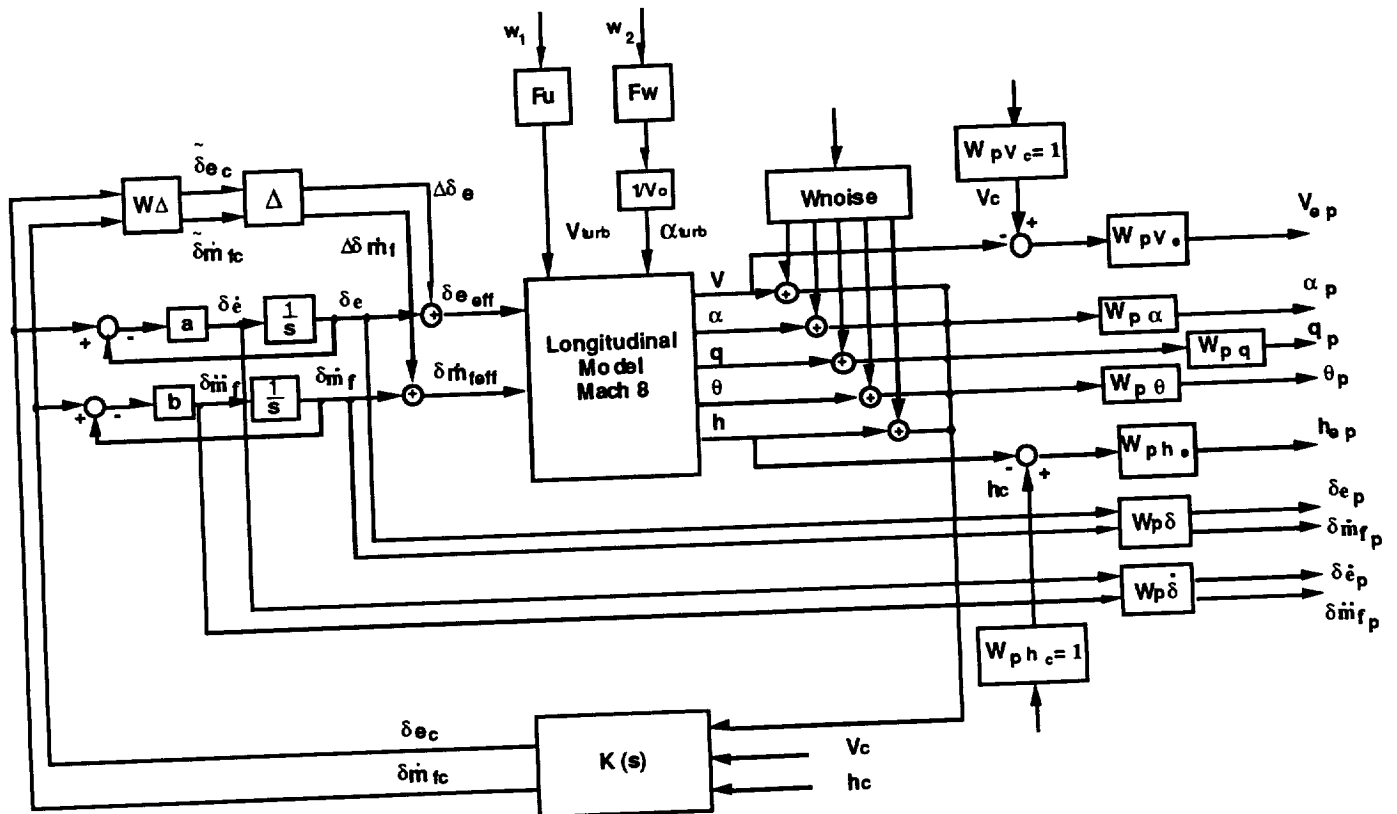


Figure 2a. Block diagram of the interconnection structure for controller design.

continuous time Dryden filters, by definition, must be divided by  $\sqrt{\text{Nyquist frequency}}$ .

The block diagram from figure 2a can be manipulated into the general framework of figure 1a as depicted in figure 2b. Recall that all the input and output signals of the generalized plant P belong to the unity bounded sets with scaling absorbed into P. In this problem the performance weighting functions also served as the scaling factors for the output signal set. Thus, the input labels in figure 2b refer to the physical quantities represented by the inputs and outputs in figure 2a. Note that the controller commanded inputs are also, after weighting, the  $\Delta$  matrix inputs, thus defining the system uncertainty. For the purpose of control synthesis the commands, atmospheric turbulence and actuator uncertainty are combined into the form given in figure 1c with the results of the controller design discussed in the following section.

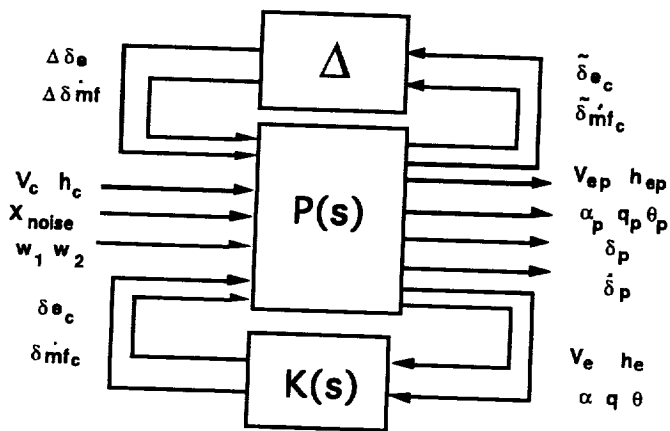


Figure 2b. Physical description of unity bounded input and output sets of generalized plant P.

### 6.0 Design Comparison

As the initial step in a controller design, an  $H_\infty$  controller for a model with no uncertainty is obtained. The nominal aircraft model is derived from the system interconnection, shown in figure 2b, by either deleting the rows and columns of P corresponding to w and z or setting  $W_\Delta = 0$ . Frequency domain closed loop system analyses for nominal performance, robust stability and robust performance are illustrated in figures 3a-b. The closed loop system using the  $H_\infty$  controller satisfies nominal performance requirements for simultaneous inputs of two tracking commands, velocity and altitude, and in the presence of

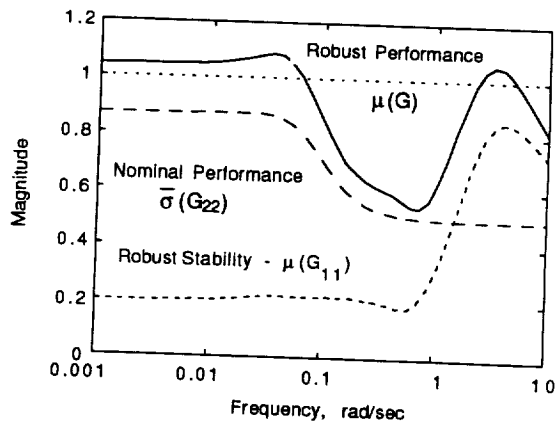


Figure 3a.  $H_\infty$  controller frequency response analysis

atmospheric turbulence in the longitudinal and vertical directions as can be seen in figure 3a. The reader will recall from section 3 that nominal performance is satisfied iff  $\bar{\sigma}(G_{22}(j\omega)) \leq 1$  for all frequency. Satisfying the nominal performance condition signifies that specified response characteristics are met for the worst possible combination of bounded inputs into the system with no uncertainty. The lack of robust performance and the contradictory results in robust stability between figures 3a and 3b, calculated with two different methods, will be addressed later.

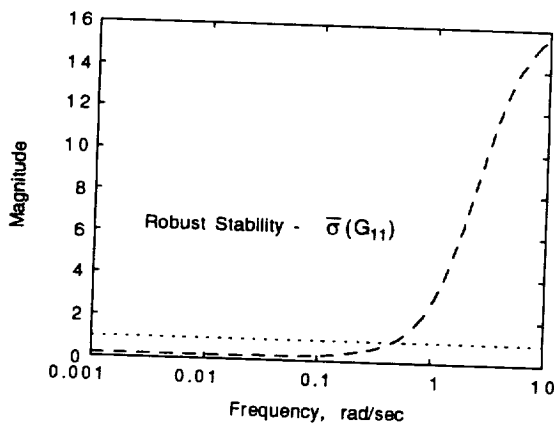


Figure 3b.  $H_\infty$  controller robust stability analysis using maximum singular value

The time response of the nominal aircraft model to simultaneous commands of 100 ft/sec velocity change and 1000 ft altitude change while encountering longitudinal and vertical atmospheric turbulence is presented in figures 4a-e. These figures also include  $\mu$  controller nominal performance which will be discussed later in this section. Both velocity and altitude, figures 4a-b, meet the performance requirements derived from tracking a near fuel optimum trajectory. The effective angle of attack experienced by the propulsion

system, shown in figure 4c, also fulfills performance specifications of less than 0.5 degree total deviation. The elevon deflection, figure 4d, is around -1 degree, thus limiting actuator induced drag. The fuel flow rate, figure 4e, avoids large sudden magnitude changes thus minimizing transients in the combustor.

Minimizing the magnitude of an actuator deflection as well as the magnitude and rate of fuel flow rate in the engine improves vehicle performance. Typically, for an airbreathing hypersonic SSTO vehicle, payload fraction is only 3 percent while fuel fraction is around 60 percent<sup>3</sup>. Therefore, any improvement in fuel fraction due to reduction in actuator induced drag has a potential to substantially increase payload fraction. Furthermore, since the performance of the propulsion system is extremely sensitive to changing conditions in the inlet, combustor and nozzle, it is important to minimize the transients in all parts of the engine. The control system minimizes perturbations in the inlet conditions by limiting angle of attack and aids combustion stability with smooth changes in fuel flow rate.

As previously mentioned, the goal of the design is to maintain performance with 20 percent control power uncertainty present in the system. Prior to dealing with robust performance, the issue of robust stability must be addressed. Two methods for stability evaluation were applied to the aircraft model depicted in figure 2a. The results of the singular value analysis,  $\bar{\sigma}(G_{11}(j\omega)) \leq 1$ , illustrated in figure 3b, indicate that the closed loop system is unstable for some  $\Delta_S$  with magnitude  $\bar{\sigma}(\Delta_S) \geq 1/16$ .

However, the  $\mu$ -analysis technique,  $\mu(G_{11}(j\omega)) \leq 1$ , which explicitly considers the block diagonal structure of the uncertainty  $\Delta$ , clearly demonstrates the stability of the same closed system in figure 3a. In fact, it becomes evident from the robust performance test that the system maintains stability and nominal performance for  $\Delta$  with a much larger magnitude than the  $\Delta_S$  that would destabilize the system according to the singular value robustness test. Furthermore, time domain plots for a perturbed closed loop system with  $H_\infty$  controller, figures 5a-g, confirm the stability of the system. The  $\Delta$  used in the time simulations was the worst-case, real-rational, stable perturbation with  $\bar{\sigma}(\Delta) \geq 1/1.1$ . The close loop poles of the perturbed system contain a complex pair that is essentially neutrally stable,  $-2.39e-10 \pm 3.91$ , and manifests itself as a harmonic like oscillation on the time plots.

Since the closed loop system is stable in the presence of structured perturbations defined in equation 5.2, the question of robust performance can now be addressed. It is evident from figure 3a that at least some performance requirements are no longer satisfied as indicated by the violation of the robust performance condition, i.e.  $\mu(G(j\omega)) > 1$ . The effect of the uncertainty on velocity and altitude, illustrated in figures 5a-b, is negligible. The most apparent difference in time response caused by the perturbations is the elevon time history. The amplitude of the perturbed response is more than twice the nominal response, figure 5e. This increased elevon activity leads directly to the poor angle of attack response depicted in figure 5c. The fuel flow rate response is also degraded significantly as indicated by the oscillations seen in figure 5g. The overall degradation in

performance is primarily a result of higher sensitivity to atmospheric turbulence. Since any elevon deflection induces significant drag, and fuel flow rate and angle of attack deviations cause a loss of propulsive performance, it would be highly beneficial to improve robust performance as much as possible in the presence of the given uncertainty.

An  $H_\infty$  controller designed with 20 percent uncertainty explicitly included in the system does not satisfy nominal performance. Figure 6 provides a sample time response of velocity to a 100 ft/sec step command. The response barely approaches 60 ft/sec velocity change which does not fulfill requirements of either steady state error or rise time. Further analysis indicates that either system uncertainty conditions or performance specifications on the tracking variables must be relaxed. Hence, an  $H_\infty$  controller cannot fulfill robust performance requirements as specified for this problem.

In an attempt to improve robust performance with original specifications, a  $\mu$  based controller is computed based on D-K iterations. The nominal performance of the  $\mu$  controller compares well with the nominal performance of  $H_\infty$  controller as illustrated in figures 4a-e. However, it is in the robust performance that the advantage of a  $\mu$  controller becomes apparent.

It is instructive to compare time response plots of the perturbed closed loop systems with  $H_\infty$  and  $\mu$  controllers as presented in figures 5a-g. The perturbed response of the  $\mu$  controller closed loop system is nearly the same as its nominal response. The performance improvements over an  $H_\infty$  controller are precisely in the variables that the former had trouble handling. The angle of attack demonstrates almost negligible response to perturbations as illustrated in figure 5d. The elevon response remains essentially unaffected by 20 percent uncertainty, figure 5f, which is also true for fuel flow rate, figure 5g. Furthermore, reducing fuel flow rate bandwidth from 100 rad/sec to 10 rad/sec to account for potential delays upstream of the controlling valves has negligible effect on the control system response.

The frequency domain analysis supports the conclusion of satisfied performance requirements in the presence of control effector uncertainty. The robust performance condition in figure 7 is met. The robust stability test results are identical for both singular value and  $\mu$  techniques. This is due to the fact that the  $\mu$  controller reflects the uncertainty structure and, thus, it is absorbed into the closed loop system. The  $\mu$  based controller successfully handles actuator uncertainty without sacrificing system performance. The encouraging preliminary results of the  $\mu$  controller establish the technique as potentially successful in dealing with unique characteristics of hypersonic class vehicles.

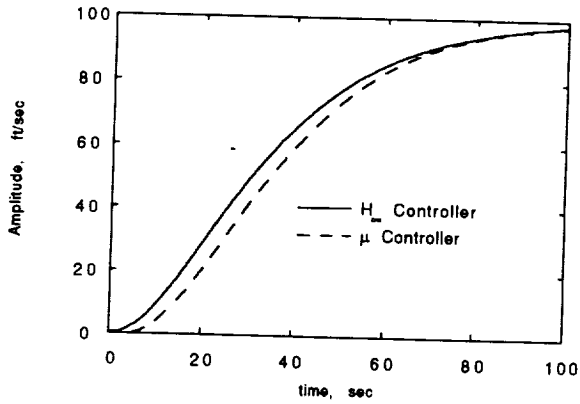


Figure 4a. Velocity response to velocity command, altitude command, vertical and longitudinal turbulence.

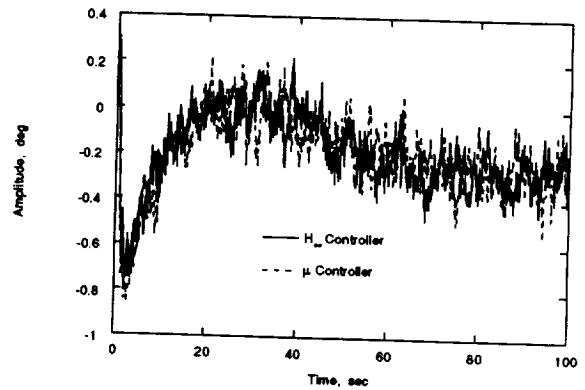


Figure 4d. Elevon response to velocity command, altitude command, vertical and longitudinal turbulence.

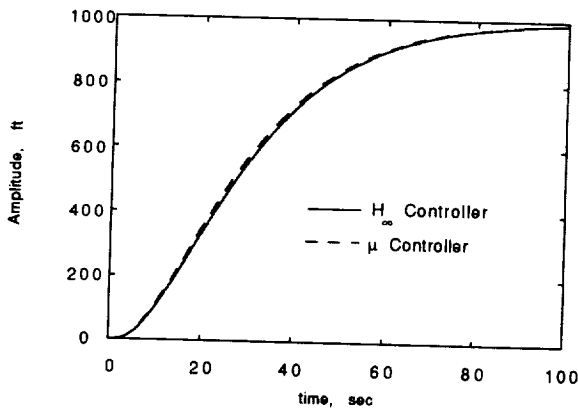


Figure 4b. Altitude response to velocity command, altitude command, vertical and longitudinal turbulence.

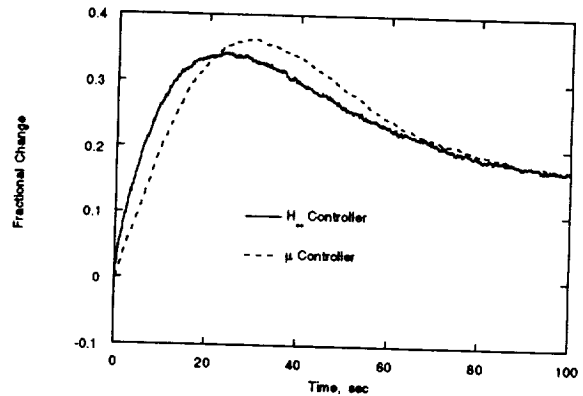


Figure 4e. Fuel flow rate response to velocity command, altitude command, vertical and longitudinal turbulence.

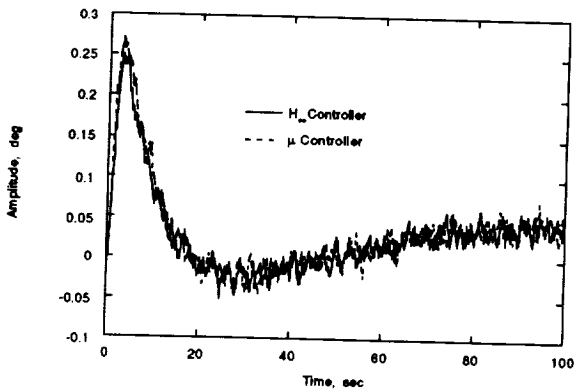


Figure 4c. Angle of attack response to velocity command, altitude command, vertical and longitudinal turbulence.

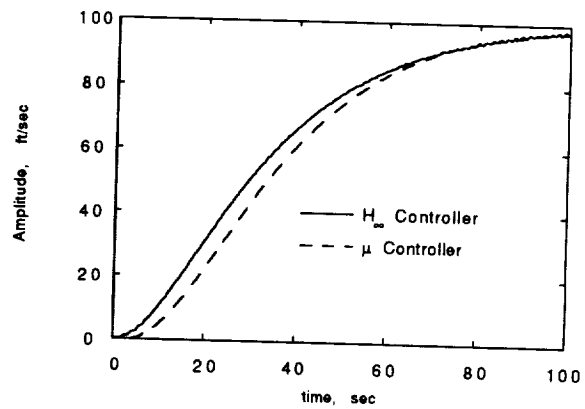


Figure 5a. Velocity response of perturbed system to velocity command, altitude command, vertical and longitudinal turbulence.

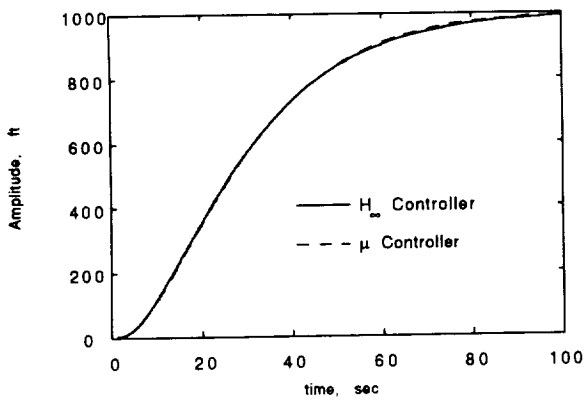


Figure 5b. Altitude response of perturbed system to velocity command, altitude command, vertical and longitudinal turbulence.

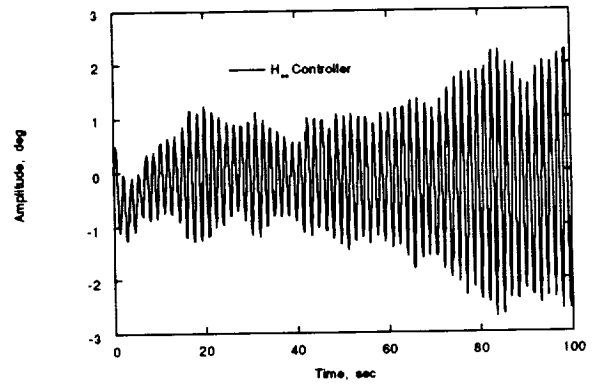


Figure 5e. Elevon response of perturbed system to velocity command, altitude command, vertical and longitudinal turbulence.

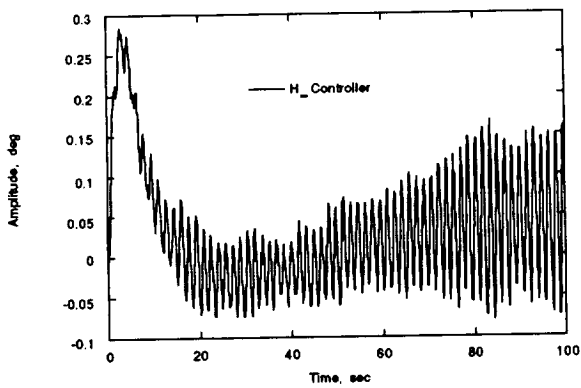


Figure 5c. Angle of attack response of perturbed system to velocity command, altitude command, vertical and longitudinal turbulence.

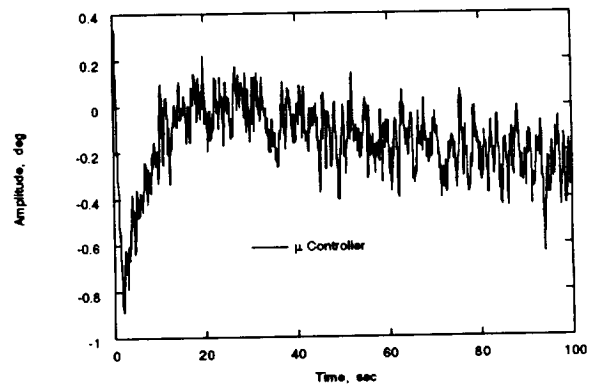


Figure 5f. Elevon response of perturbed system to velocity command, altitude command, vertical and longitudinal turbulence.

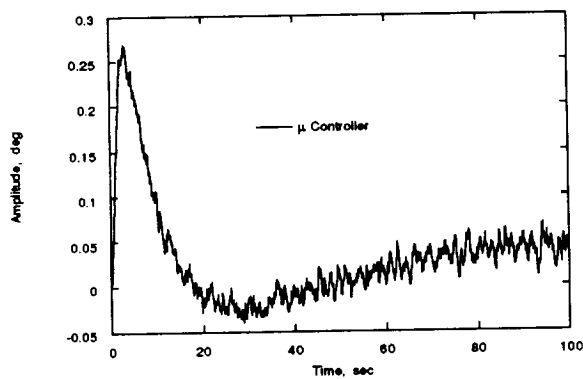


Figure 5d. Angle of attack response of perturbed system to velocity command, altitude command, vertical and longitudinal turbulence.

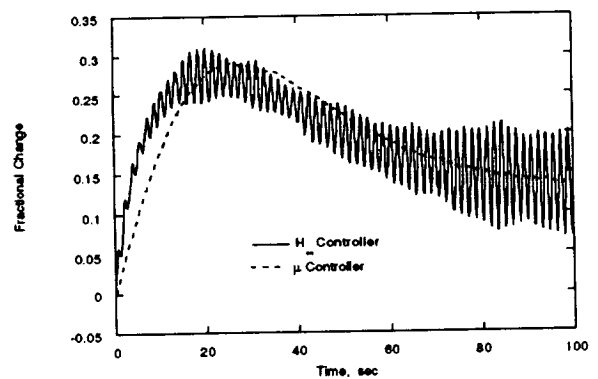


Figure 5g. Fuel flow rate response of perturbed system to velocity command, altitude command, vertical and longitudinal turbulence.

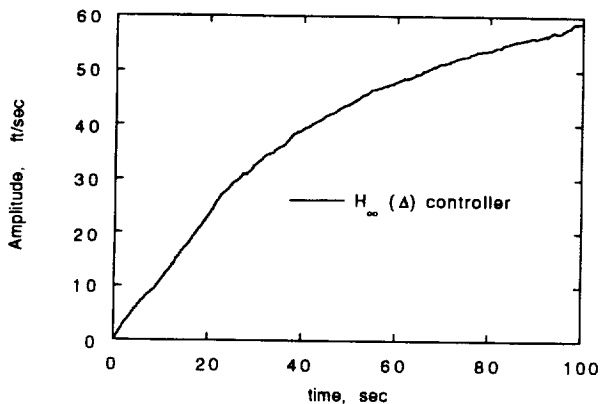


Figure 6. Velocity response to velocity command, altitude command, vertical and longitudinal turbulence of a system with an  $H_{\infty}$  controller designed explicitly with uncertainty.

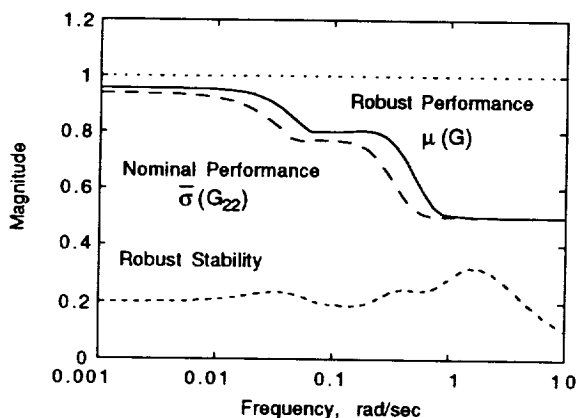


Figure 7.  $\mu$  controller frequency response analysis

## 7.0 Conclusions

Applicability of robust control techniques to an SSTO airbreathing hypersonic vehicle on an ascent accelerating path and their effectiveness are explored in this paper. Several important issues related to control system design should be noted. The most important results are based on comparison between  $H_{\infty}$  and  $\mu$  techniques. Since uncertainty plays an integral part of hypersonic vehicle characteristics, its effect on the analysis and synthesis of various control system design techniques is important to understand.

The characteristics describing airbreathing hypersonic vehicles and the requirements imposed on the control system translate explicitly into  $H_{\infty}$  domain specifications as illustrated in this paper. However, the  $H_{\infty}$  controller suffers performance degradation with introduction of control effector uncertainty into the system. The  $\mu$  controller preserves the

required performance while providing stability robustness. Hence,  $\mu$  synthesis, by taking into consideration the structure of the uncertainty in this problem, results in an improved robust performance over the  $H_{\infty}$  controller. As previously mentioned the extent of conservatism induced by singular value robustness analysis varies considerably from problem to problem. In this typical hypersonic problem formulation, singular value analysis is conservative for a relatively benign control effector uncertainty.

The cumulative results of this research imply the importance of  $\mu$  as both the analysis and the synthesis tool for an airbreathing hypersonic vehicle. Since uncertainty occurs simultaneously from many different sources and the degree of uncertainty is high, the physical behavior of the system introduces structure into the problem. It is essential to employ a methodology that takes full advantage of these physical characteristics. The  $\mu$ -analysis and synthesis technique preserves the structural relationship between uncertainty and performance variables, allowing the designer a systematic approach to explore tradeoffs between the two. Failure to account for this structural relationship can result in excessively conservative specifications and poor designs for an airbreathing hypersonic vehicle.

## References

1. Shaughnessy, John D.; John D. McMinn; Irene M. Gregory; Rajiv S. Chowdhry; David L. Raney, and Frederick J. Lallman. "Controls, Guidance and Trajectory Integration Issues for NASP." 10th National Aero-Space Plane Symposium, Monterey, California, April 1991.
2. Walton, J. "Performance Sensitivity of Hypersonic Vehicles to Changes in Angle of Attack and Dynamic Pressure." AIAA Paper No. 89-2463, 1989.
3. Wilhite, Alan; Richard Powell; Stephen Scotti; Charles McClinton; S. Zane Pinckney; Christopher Cruz; L. Robert Jackson, and James Hunt. "Concepts Leading to the National Aero-Space Plane Program." 28th Aerospace Sciences Meeting, Reno, Nevada, January 1990.
4. Cribbs, D. "Performance Uncertainty Analysis for NASP." AIAA Paper No. 90-5209.
5. Shaughnessy, John D., and Irene M. Gregory. Trim Drag Reduction Concepts for Horizontal Takeoff Single-Stage-To-Orbit Vehicles. NASA TM 102687, December 1991.
6. McRuer, Duane T.; Irving L. Ashkenas, and Donald E. Johnston. Hypersonic Technology Planning: Flying Qualities and Control Issues/Features for Hypersonic Vehicles. Technical Report No. 2361-1 (Subcontract ATD-88-STI0221), May 1989.
7. Anderson, Mark R., and Abbas Emami-Naeini. "Robust Control Law Development for a Hypersonic Cruise